JGR Oceans

RESEARCH ARTICLE
10.1029/2020JC016258

Key Points:
- Typhoons tend to have a three-step effect on surface pCO_2: first cooling, followed by mixing, and then potentially biological uptake
- Increased air-sea CO_2 flux during typhoon effect periods is caused primarily by high wind speed
- Typhoons enhance CO_2 efflux by 23–56% in the northern South China Sea during the last decade

Correspondence to:
P. Yu and Z. A. Wang,
yuppe@sio.org.cn;
zawang@whoi.edu

Citation:
Yu, P., Wang, Z. A., Churchill, J., Zheng, M., Pan, J., Bai, Y., & Liang, C. (2020). Effects of typhoons on surface seawater pCO_2 and air-sea CO_2 fluxes in the northern South China Sea. *Journal of Geophysical Research: Oceans*, *125*, e2020JC016258. https://doi.org/10.1029/2020JC016258

Received 19 MAR 2020
Accepted 28 JUL 2020
Accepted article online 3 AUG 2020

Effects of Typhoons on Surface Seawater pCO_2 and Air-Sea CO_2 Fluxes in the Northern South China Sea

Peisong Yu[1], Zhaohui Aleck Wang[2], James Churchill[3], Minhui Zheng[1], Jianming Pan[1], Yan Bai[4], and Chujin Liang[4]

[1]Key Laboratory of Marine Ecosystem Dynamics, Second Institute of Oceanography, Ministry of Natural Resources, Hangzhou, China, [2]Department of Marine Chemistry and Geochemistry, Woods Hole Oceanographic Institution, Woods Hole, MA, USA, [3]Department of Physical Oceanography, Woods Hole Oceanographic Institution, Woods Hole, MA, USA, [4]State Key Laboratory of Satellite Ocean Environment Dynamics, Second Institute of Oceanography, Ministry of Natural Resources, Hangzhou, China

Abstract This study assessed the effects of typhoons on sea surface pCO_2 and CO_2 flux in the northern South China Sea (SCS). During the passage of three major typhoons from May to August 2013, sea surface pCO_2, surface seawater temperature (SST), and other meteorological parameters were continuously measured on a moored buoy. Surface water in the region was a source of CO_2 to the atmosphere with large variations ranging from hours to months. SST was the primary factor controlling the variation of surface pCO_2 through most of the time period. Typhoons are seen to impact surface pCO_2 in three steps: first by cooling, thus decreasing surface pCO_2, and then by causing vertical mixing that brings up deep, high-CO_2 water, and lastly triggering net uptake of CO_2 due to the nutrients brought up in this deep water. The typhoons of this study primarily impacted air-sea CO_2 flux via increasing wind speeds. The mean CO_2 flux during a typhoon ranged from 3.6 to 5.4 times the pretyphoon mean flux. The magnitude of the CO_2 flux during typhoons was strongly inversely correlated with the typhoon center distance. The effect of typhoons accounted for 22% of the total CO_2 flux in the study period, during which typhoons occurred only 9% of the time. It was estimated that typhoons enhanced annual CO_2 efflux by 23–56% in the northern SCS during the last decade. As such, tropical cyclones may play a large and increasingly important role in controlling CO_2 fluxes in a warmer and stormier ocean of the future.

Plain Language Summary The global ocean absorbs about 25% of anthropogenic carbon dioxide emissions from the atmosphere and plays an important role in regulating global climate. One important question regarding estimates of carbon dioxide flux at the ocean surface is how episodic events such as typhoons affect surface seawater carbon dioxide and air-sea carbon dioxide exchange. In this study, seawater temperature generally played a primary role in controlling surface seawater carbon dioxide under nontyphoon conditions in the northern South China Sea. We found that typhoons seem to have a three-step effect on surface carbon dioxide: first cooling, which decreases carbon dioxide content, followed by vertical mixing that can bring up deep water with high concentrations of carbon dioxide and nutrients, and lastly the triggering of net uptake of carbon dioxide due to phytoplankton growth fueled by those nutrients. Increased air-sea carbon dioxide flux during a typhoon is caused primarily by high wind speed. Typhoons enhanced carbon dioxide flux to the atmosphere by 23–56% annually in the study region. As such, typhoons may play a more important role in the control of carbon dioxide fluxes in a warmer and stormier ocean of the future.

1. Introduction

The global ocean absorbs about 1.6–2.0 Pg C $year^{-1}$ from the atmosphere, corresponding to about 25% of anthropogenic CO_2 emissions (Iida et al., 2015; Takahashi et al., 2009; Wanninkhof et al., 2013). This estimate is relatively well constrained based on a compilation of directly measured oceanic CO_2, obtained primarily from shipboard underway and in situ time series measurements. Measurements of pCO_2 in coastal oceans have increased dramatically in recent decades. However, the estimates of CO_2 fluxes in coastal systems still bear large uncertainties due to significant heterogeneity, and limited spatiotemporal coverage, of these fluxes (Bauer et al., 2013; C. T. A. Chen et al., 2015; Laruelle et al., 2014). The current understanding is that global continental shelves serve as a CO_2 sink, while near-shore systems and estuaries are CO_2

sources (Bauer et al., 2013; Cai et al., 2006; Cai et al., 2011; C. T. A. Chen & Borges, 2009; Dai et al., 2013). Accurate assessment of the air-sea CO_2 flux, and its spatiotemporal variability, in the coastal ocean is needed to improve the understanding of the coastal carbon cycle and to predict future changes in coastal systems and the complex biogeochemical impacts of these changes, including coastal ocean acidification.

An important question regarding estimates of CO_2 fluxes in the ocean is how episodic events such as storms affect surface pCO_2 and air-sea CO_2 exchange. The effects of such events have not been well quantified in estimates of CO_2 fluxes. In addition to their possible effect on CO_2 fluxes, storms can potentially modify carbon biogeochemistry. For example, nutrients upwelled during storms may trigger phytoplankton blooms, altering the Biological Carbon Pump, a process that has not been well assessed on regional and global scales. Understanding the influence of storms on marine carbon biogechemistry is important to better constrain oceanic CO_2 fluxes and to predict future changes in these fluxes, given that storm intensity may increase under climate change (Intergovernmental Panel on Climate Change, IPCC, 2013).

Evidence of the impact of storms on CO_2 fluxes at the ocean surface has come from a number of studies. Based on shipboard observations made before and after the passage of hurricanes, Bates et al. (1998) showed that hurricanes increased the summertime CO_2 efflux by nearly 55% in the Sargasso Sea. Hood et al. (2001) observed a sharp decrease in surface seawater temperature (SST), as well as increases in pCO_2 and nitrate concentrations, during a storm with wind speeds reaching 16–17 m s^{-1}. The CO_2 flux during the storm doubled due to the elevated wind speed. Nemoto et al. (2009) found that three typhoons accounted for 60% of the summertime efflux of CO_2 in the western subtropical North Pacific. Surface pCO_2 was likely impacted by vertical turbulent mixing and upwelling resulting from the typhoons. Evidence that episodic events, such as typhoons, can have large effects on air-sea CO_2 exchange has also been reported by Huang and Imberger (2010) and Sun et al. (2014). However, with a few exceptions, most previous studies were based on short-term observations (days to weeks) around typhoon periods, or on numerical simulation (Koch et al., 2009). As such, understanding of the effects of typhoons on pCO_2 and CO_2 fluxes over monthly to seasonal scales and beyond is presently limited. Long-term (encompassing a number of typhoons as well as quiescent between typhoons) and high-resolution time series pCO_2 measurements, along with other relevant observations, are key to assess the impact of typhoons on CO_2 fluxes over these longer scales. In addition, more dedicated studies are necessary to improve understanding of the mechanisms controlling surface pCO_2 and impacting CO_2 fluxes during storms. Such knowledge is key to establishing mechanistic models to evaluate storm effects on pCO_2 and CO_2 fluxes at the ocean surface.

With a total area of approximately 2.5×10^{-6} km^2, the South China Sea (SCS) is the largest tropical marginal sea in the western Pacific Ocean. Observations of surface pCO_2 in the SCS show spatiotemporal variability in the range of 280 to 470 μatm and suggest that the SCS as a whole serves as a weak to moderate source of CO_2 to the atmosphere (3.1 ± 1.7 mmol m^{-2} day^{-1}) (C. T. A. Chen et al., 2006; Dai et al., 2013; Zhai et al., 2005, 2013). Zhai et al. (2013) found that the northern SCS also served as a weak CO_2 source with an annual air-sea CO_2 flux of 1.3 ± 1.2 mmol m^{-2} day^{-1}. However, earlier studies based on time series observations at the South-East Asian Time Series Study station (SEATS, 18°15′N, 115°35′E) found that the northern SCS was a weak CO_2 sink, removing 0.05–0.5 mmol m^{-2} day^{-1} from the atmosphere (Chou et al., 2005; Tseng et al., 2007). Since these studies are all several years in duration, the discrepancy suggests interannual variability of the CO_2 flux in the northern SCS.

On a seasonal scale, the study of Zhai et al. (2013) showed that offshore surface water of the northern SCS releases CO_2 to the atmosphere in spring (1.7 ± 0.8 mmol m^{-2} day^{-1}, surface pCO_2 ranging from 363 to 444 μatm), becomes a stronger CO_2 source in summer (3.2 ± 0.3 mmol m^{-2} day^{-1}, pCO_2 from 353 to 421 μatm), and has air-sea CO_2 exchanges that are nearly in equilibrium in autumn (1.0 ± 1.8 mmol m^{-2} day^{-1}, pCO_2 from 345 to 411) and winter (−0.9 ± 1.9 mmol m^{-2} day^{-1}, pCO_2 from 324 to 398 μatm). In general, SST is the major factor controlling the seasonal variation of surface pCO_2 in offshore areas, while biological effects seem to be secondary (Tseng et al., 2007; Zhai et al., 2005, 2013). On a shorter time scale, surface seawater pCO_2 in these offshore waters shows a small diel change, on the order of ~10 μatm (Dai et al., 2009).

Due to a relatively stable and deep mixed-layer depth (~44 m), vertical mixing has a limited effect on surface seawater pCO_2 in the offshore SCS region (Dai et al., 2009). The northern SCS is also occasionally influenced by an intrusion of the Kuroshio Current via the Luzon Strait (C. T. A. Chen et al., 2001; Dai et al., 2013;

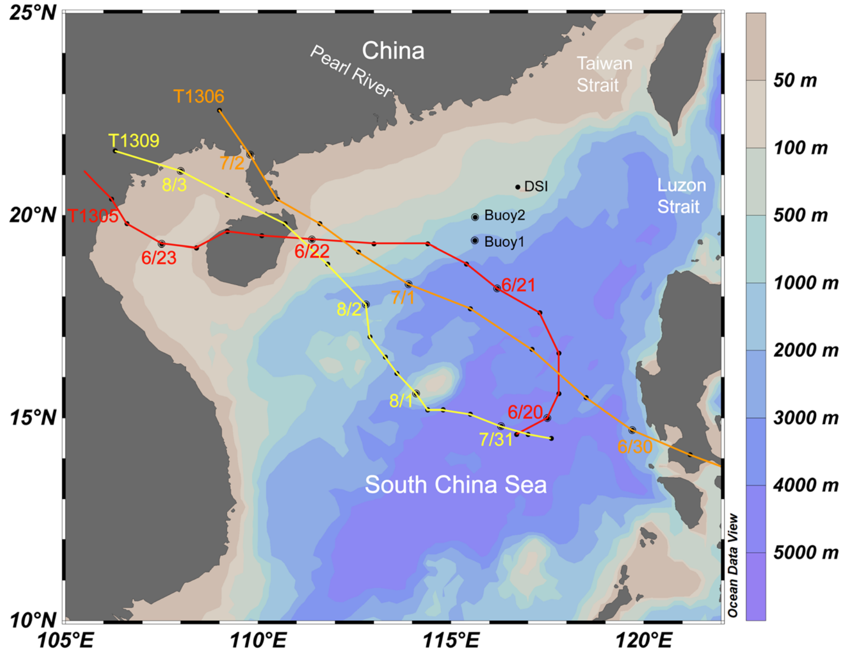

Figure 1. The northern South China Sea and vicinity with the tracks of three major typhoons in 2013. The locations of two buoy sites are marked as black dots. Colored lines represent the tracks of the three typhoons (T1305, T1306, and T1309). Dots along the track lines indicates a typhoon's location every 6 hr. DSI denotes Dongsha Island where atmospheric xCO_2 was measured. Water depth is indicated by the color bar on the right. Map was produced with Ocean Data View software (https://odv.awi.de).

Du et al., 2013), which can generate mesoscale cyclonic eddies in the northeast monsoon season (Sheu et al., 2010). This process may pump water enriched in nutrients and CO_2 from the depths to the surface, causing phytoplankton blooms (He et al., 2016; Shang et al., 2012).

In the nearshore region of the northern SCS, the air-sea CO_2 exchange is small (i.e., near equilibrium) in spring (0.4 ± 1.6 mmol m^{-2} day^{-1}), summer (-0.6 ± 1.1 mmol m^{-2} day^{-1}), and autumn (0.2 ± 1.9 mmol m^{-2} day^{-1}) (Zhai et al., 2013). However, the region is a moderate CO_2 sink in winter (-4.8 ± 2.6 mmol m^{-2} day^{-1}). As such, the annual air-sea CO_2 flux is close to zero (-1.2 ± 1.8 mmol m^{-2} day^{-1}) (Zhai et al., 2013). In addition to SST, other factors can impose high variability on surface pCO$_2$ distribution in the nearshore region. The Pearl River plume in flooding seasons and seasonal upwelling along the southern China coast can have profound impacts on nearshore biogeochemical processes in the northern SCS (Bai et al., 2015). Each of these processes contributes significant inputs of nutrients to the coastal waters, inducing substantial drawdown of surface pCO$_2$ through enhanced primary productivity (Cao et al., 2011; Dai et al., 2008).

To the best of our knowledge, no studies have investigated the effects of typhoons and other episodic events on surface pCO$_2$ and air-sea CO_2 flux in the northern SCS. Using extended in situ time series measurements in the SCS, this study explicitly examines and evaluates the effects of the passage of typhoons on surface seawater pCO$_2$ and air-sea CO_2 flux. We focus on characterizing and evaluating how biogeochemical and physical processes, such as cooling, mixing, and biological activity triggered by typhoons, impact surface pCO$_2$, and CO_2 flux, thus improving our understanding of the impact of typhoons on carbon biogeochemistry. We also assess the impact of typhoons on overall CO_2 flux in the northern SCS during the last decade. The results provide insights on the factors controlling CO_2 flux at the study site. We compare these results with findings from other regions in order to examine the similarities and differences in the tropical storm effects across sites.

2. Materials and Methods

2.1. Study Site

The northern SCS is bordered by the mainland of China to the north and by the deep SCS basin to the south (Figure 1). It has a wide shelf extending 150 to 300 km offshore. The shelf system receives freshwater influx mainly from the Pearl River, which is the thirteenth among world rivers when ranked by discharge (3.26×10^{11} m^3 $year^{-1}$), with 80% of this influx occurring in the wet season from April to September (Guo et al., 2008; Su, 2004). The climate in the northern SCS is dominated by the Asian monsoon. The rain-bearing southwest monsoon lasts from June to September, while the northeast monsoon, typically characterized by higher wind speed, prevails from November to March, with a transition period from March to June (Han, 1998). Coastal upwelling often occurs in summer, driven by the prevailing southwest monsoon (Han & Ma, 1988). The northern SCS slope area is typically oligotrophic (Wong et al., 2007) and low in productivity (Y. L. L. Chen & Chen, 2006). However, phytoplankton productivity on both the shelf and slope in the northern SCS can be enhanced by the Pearl River plume and mesoscale eddies (He et al., 2016). The SCS experiences frequent typhoons, on average of more than seven annually, triggering sea surface cooling and phytoplankton blooms due to mixing and upwelling (Chang et al., 2008; C. T. A. Chen et al., 2003; Lin et al., 2003; Zhao et al., 2008).

2.2. Measurements

Surface water pCO_2 was measured hourly using a SAMI-CO_2 sensor (Sunburst Inc., Missoula, MT, USA) mounted on a buoy moored in the northern SCS over 94 days in 2013 (Figure 1). The buoy was first deployed at 115°37′18″E, 19°22′55″N (Buoy 1 in Figure 1, water depth 2,610 m) from 8 May through 28 June 2013. It was then serviced and redeployed at a nearby site (115°37′35″E, 19°57′11″N, Buoy 2 in Figure 1, water depth 1,470 m) from 28 June through 10 August 2013. The buoy sites, separated by 64 km, were near the slope of the northern SCS (Figure 1). The nominal measurement range of the SAMI-CO_2 sensor is between 150 and 700 μatm, with a manufacturer's reported accuracy of about ±1 μatm. Before deployment, the sensor was calibrated in the laboratory against a flow-through pCO_2 system (General Oceanics, Model G8050). The two systems were found to be in good agreement with a mean difference of 3.1 ± 2.5 μatm ($n = 9$). The SAMI-CO_2 sensor was located below the sea surface at ~1 m in depth and was covered with copper mesh.

Wind speed and SST were obtained hourly from the meteorological sensors on the buoy. All buoy data were sent through iridium satellite to the laboratory at the Second Institute of Oceanography, Hongzhou, China, in real time. All data are reported in local time, as this is useful for discussion of effects of biological activities. During the study period, local sunrise and sunset times at the buoy site were ~6 a.m. and ~7 p.m., respectively. The typhoon track data used in this paper (Figure 1) were obtained from the U.S. Joint Typhoon Warning Centre (JTWC, http://www.usno.navy.mil/JTWC/). The data include the location and intensity of the typhoon centers at 6-hr intervals. Atmospheric CO_2 mole fraction (in dry air, xCO_2^{air}) was measured at the Dongsha Island (DSI) monitoring site (https://www.esrl.noaa.gov/gmd/dv/data/index.php), located in the northern SCS at 116°43′47″E, 20°41′57″N, about 200 km northeast of the buoy sites (Figure 1). xCO_2^{air} was measured weekly from May to August 2013. To estimate air-sea CO_2 flux, atmospheric pCO_2 (pCO_2^{air}) was calculated from xCO_2^{air}, SST and salinity.

2.3. Air-Sea CO_2 Flux

Air-sea CO_2 flux (F) was calculated using the gas transfer velocity (k), the pCO_2 gradient between sea surface (pCO_2^{sea}) and overlying air (pCO_2^{air}) as follows:

$$F = k \times K_H \times \left(pCO_2^{sea} - pCO_2^{air}\right) \tag{1}$$

where K_H is the solubility of CO_2 in seawater (Weiss, 1974). Positive F corresponds to a flux from ocean to atmosphere, meaning the ocean is an air-sea CO_2 source to the atmosphere. In this study, we used four published k parameterizations based on wind speed at 10 m above sea surface (U_{10}) to calculate fluxes:

$$k = 0.31 \times {U_{10}}^2 \times (S_c/660)^{-0.5} \tag{2}$$

(Wanninkhof, 1992)

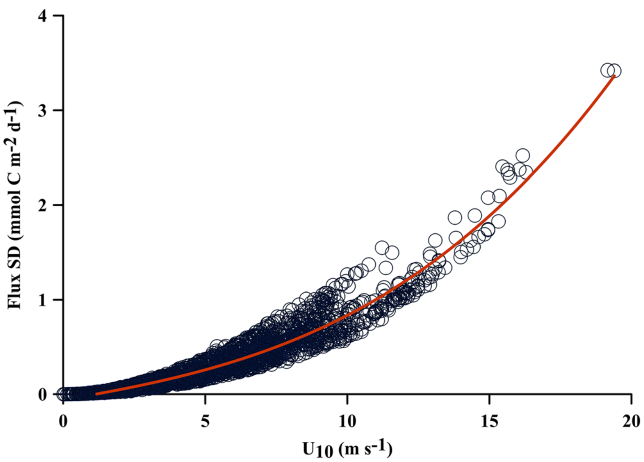

Figure 2. Standard deviation (SD) of calculated mean CO_2 fluxes based on four different k parameterizations (see text) as a function of U_{10}. Red line is regression curve.

$$k = 0.266 \times U_{10}{}^2 \times (S_c/660) - {}^{0.5} \tag{3}$$

(Ho et al., 2006)

$$k = 0.27 \times U_{10}{}^2 \times (S_c/660)^{-0.5} \tag{4}$$

(Sweeney et al., 2007)

$$k = 0.251 \times U_{10}{}^2 \times (S_c/660)^{-0.5} \tag{5}$$

(Wanninkhof, 2014) where S_c is the Schmidt number for CO_2 in seawater. These equations have been frequently used in marine CO_2 studies. Equations 2 and 4 were also used to estimate air-sea CO_2 flux in the SCS in previous study (Zhai et al., 2013). Equation 5 is an update on the widely used method by Wanninkhof (1992). Herein, we report mean flux values calculated from the above four equations with one standard deviation (SD). The rational is that the averaged k represents the largest number of relevant independent observations used to derived these equations and thus better reflects the real uncertainty of k (as compared with the k produced by a single parameterization).

In this study, an AIRMAR wind sensor (Model 150WX) was deployed on the mooring at ~3 m above the sea surface. Wind speed was converted to U_{10} using the equation derived by Large and Pond (1981):

$$U_{10} = U_Z / \left(1 + \frac{\sqrt{Cd_{10}}}{0.4} \times \ln\left(\frac{Z}{10}\right)\right) \tag{6}$$

where Z is the height (m) above sea surface (3 m in this study), U_Z is wind speed (m s^{-1}) measured at Z, Cd_{10} is the drag coefficient (0.0011), and 0.4 is von Karman's constant. U_{10} was based on gust wind speed.

To evaluate effects of typhoons on surface pCO_2 and CO_2 flux, the typhoon effect period (TEP) was defined as the period that starts when U_{10} was 30% higher than the mean value in the previous 24 hr and ends when U_{10} returned to its starting value before the typhoon's passage. This definition captured the periods when the U_{10} was elevated by typhoons, though it is somewhat arbitrary as there is no established definition for TEP.

2.4. Uncertainty of Air-Sea CO_2 Flux Calculation

The major uncertainty of the air-sea CO_2 flux calculation is due to k parameterization, which has an estimated uncertainty of 20% when $U_{10} > 3$ m/s (Wanninkhof, 2014). At low winds, nonwind effects such as chemical enhancement and thermal boundary layer processes influence gas transfer, and the quadratic relationship will underestimate gas transfer velocity (Wanninkhof, 2014). In this study, we evaluated the variability of CO_2 flux by using different k parameterizations (Equations 2–5). When $U_{10} < 6$ m s^{-1}, the condition during most of the nontyphoon periods (Figure 2), the SD of mean CO_2 flux calculated from the four equations ranged from 0 to 0.5 mmol m^{-2} day^{-1} with a mean of 0.2 mmol m^{-2} day^{-1}. The SD increased to 0.5–3.4 (with a mean of 1.0) mmol m^{-2} day^{-1} when $U_{10} > 9$ m s^{-1}, which was the predominant condition during TEPs. The maximum SD of 3.4 mmol m^{-2} day^{-1} occurred when U_{10} reached 19.4 m s^{-1}, corresponding to an air-sea CO_2 flux of 41.7 mmol m^{-2} day^{-1} (Figure 2). The relative SD of CO_2 fluxes across all wind speeds was ~8%. These uncertainties do not affect our interpretation of the effects of typhoons on CO_2 flux, as the cumulative CO_2 flux during typhoons accounts for 22% of CO_2 fluxes during the study period (see section 3.3) or 23–56% of the annual CO_2 flux during 2008–2018 (see section 3.4).

Another uncertainty may result from using the weekly measurement of $xCO_2{}^{air}$, while the pCO_2 data have higher (hourly) resolution. We used linear interpolation to convert the weekly $xCO_2{}^{air}$ data to hourly values for the flux calculation. We estimated the potential uncertainty of using weekly $xCO_2{}^{air}$ data by examining the daily $xCO_2{}^{air}$ data measured in Hawaii (Site MLO, 19°32′10″N, 155°34′34″W, https://www.esrl.noaa.gov/gmd/dv/data/index.php). Daily $xCO_2{}^{air}$ at MLO ranged between 395.27 and 400.39 ppm during the period of 8 May through 10 August 2013 when our measurements took place. The differences between this daily

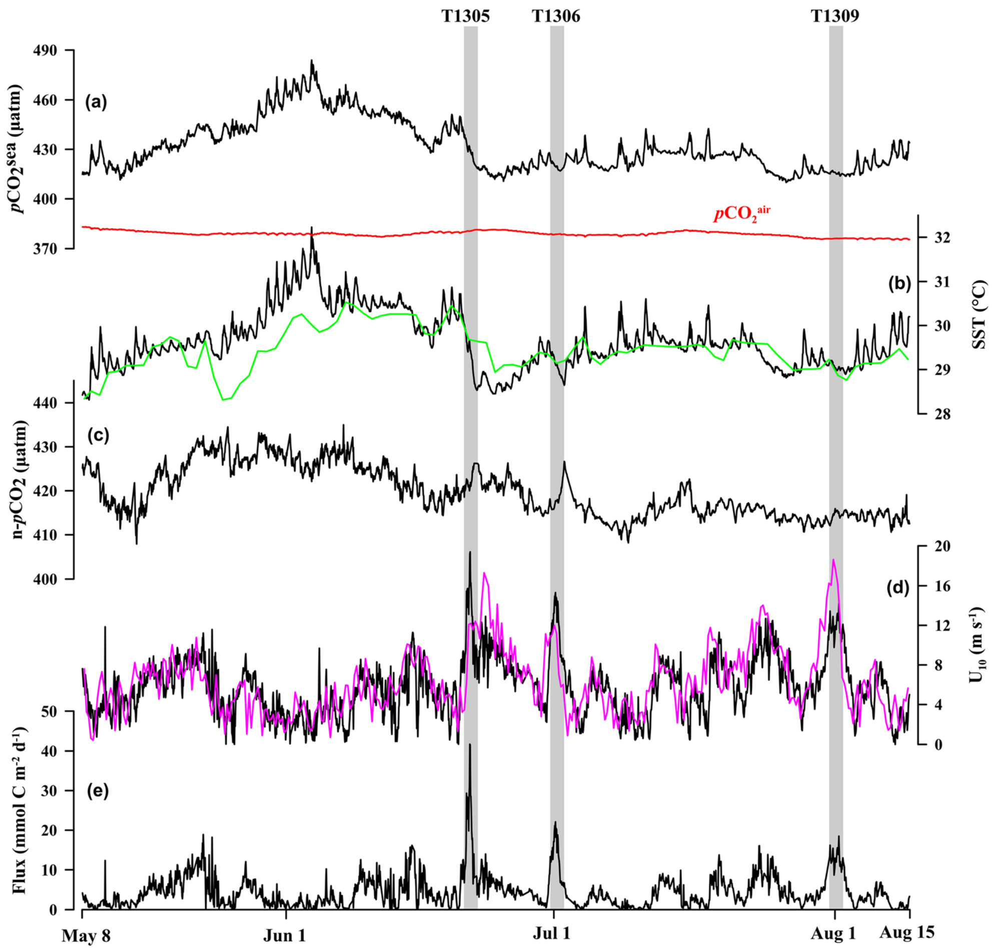

Figure 3. Variations of surface pCO_2 (a), SST (b), *n*-pCO_2 (c), U_{10} (d), and CO_2 flux (e) in the northern SCS from 8 May to 10 August in 2013. pCO_2 (a), SST (b), and U_{10} (d) were measured in situ hourly. Gray areas represent the periods of three typhoons passing by. Green line represents SST data from ERSL. Purple line represents U_{10} data from NCEP.

xCO_2^{air} series and a daily series determined by taking weekly xCO_2^{air} points and interpolating them to hourly values varied from −0.86 to 0.74 ppm. Such differences are only ~0.2% of the mean xCO_2^{air} (398.21 ppm) during the period. At the mean wind speed and mean pCO_2 observed in this study, this translates to a CO_2 flux uncertainty of ~0.06 mmol C m^{-2} day^{-1} or ~1.5%, which is insignificant in our flux calculations.

3. Results and Discussion

3.1. Surface Variability

Hourly measured sea surface pCO_2 showed high variability over multiple time scales in the northern SCS from early May through August 2013 (Figure 3a). pCO_2 generally trended closely with SST (Figure 3b), following a significant relationship of $pCO_2 = (369 \pm 19\ \mu atm) \times e^{0.0423\ (SST\text{-}26)}$ ($n = 2{,}049$, $r^2 = 0.876$), where 26 is the annual average SST of the offshore water in °C (Zhai et al., 2005). This is nearly identical to a SST-pCO_2 relationship derived from underway observations in the northern SCS by Zhai et al. (2005). From early May through early June, pCO_2 gradually increased with rising water temperature, primarily the result of increased solar heating. Subsequently, pCO_2 exhibited a decreasing trend until late June (Figure 3a) and showed less variation thereafter. The maximum pCO_2 value of 484 µatm occurred on 3 June, which corresponded to a SST maximum of 32.23°C. The minimum pCO_2 of 410 µatm was observed on 27 July, while the minimum SST value of 28.31°C occurred on 9 May. The mean (±SD) pCO_2 was 432 ± 15 µatm ($n = 2{,}049$) during the study period.

pCO_2^{air} had a mean value of 379 μatm from May through August with little variation (±2 μatm) (Figure 3a). Air-sea pCO_2 difference, ΔpCO_2, defined as $pCO_2^{sea} - pCO_2^{air}$, ranged from 29 to 106 μatm with a mean of 53 ± 16 μatm. The region was a CO_2 source to the atmosphere during the entire study period.

SST showed limited variation, with a mean of 29.66 ± 0.66°C ($n = 2{,}216$) during the study period (Figure 3b). To control for the effect of temperature, pCO_2 was normalized to $T = 29$°C (close to mean SST) as n-pCO_2, which was confined within a narrow range of 420 ± 6 μatm ($n = 2{,}049$) from May through August (Figure 3c), even though the study period covered a major portion of the production season. Overall, surface variability of pCO_2 measured at the buoy site is representative of an oligotrophic nonupwelling system, where the thermal effect primarily controls surface pCO_2 and the biological effect is limited. Such a condition resulted in the ocean being a net weak CO_2 source during the study period. The study site thus bears the characteristics of a tropical/subtropical shelf region in terms of air-sea CO_2 fluxes (Cai et al., 2006).

During the study period of 8 May to 10 August 2013, five typhoons passed through the northern SCS. Among these typhoons, three (T1305-Bebinca, T1306-Rumbia, and T1309-Jebi) passed south of the buoy sites at a nearest distance from 69 to 382 km (Figure 1). They had appreciable effects on U_{10} at buoy sites (Figure 3d). The effects of the other two typhoons were relatively small and will not be discussed. Rapid increase of U_{10} and decrease of pCO_2 and SST were observed during the three TEPs (gray area in Figure 3). This suggests that typhoons may have a large effect on SST, U_{10} and pCO_2 and thus on air-sea CO_2 flux.

U_{10} measured at times other than the typhoon events was generally below 8 m s^{-1} with an average of 5.3 ± 2.5 m s^{-1}. During each typhoon event, U_{10} at the buoy site sharply increased and reached a maximum value as high as 19.4 m s^{-1} (Figure 3d). U_{10} decreased to a normal range within 1 to 2 days after each typhoon event. The air-sea CO_2 flux was mostly below 10 mmol C m^{-2} day^{-1} outside TEPs (Figure 3e). The mean CO_2 flux during the entire study period was 4.6 ± 4.2 ($n = 2{,}020$) mmol C m^{-2} day^{-1}. However, the mean flux during TEPs was 12.3 ± 6.7 ($n = 166$), with the highest flux of 41.7 ± 3.4 mmol C m^{-2} day^{-1} occurring during Typhoon T1305 (Figure 3e).

3.2. Effects of Typhoons on pCO_2

The buoy data revealed significant variations in pCO_2 at time scales ranging from hours to months. The most pronounced temporal changes in pCO_2 were associated with the passage of typhoons. Three typhoons passed the area near the buoy from June to August 2013, all significantly impacting pCO_2 and CO_2 fluxes (Figures 1 and 3). The three typhoons affected pCO_2 in similar and contrasting ways, which are detailed in the following sections.

3.2.1. Typhoon Bebinca (T1305, 21–24 June 2013)

Typhoon Bebinca (T1305) formed in the central SCS on 20 June and passed south of the buoy site on 21 June (Figure 1). The nearest distance between the typhoon center and the buoy site was ~69 km (Table 1). On 19–20 June, before the passage T1305, U_{10} was low (%3C m s^{-1}), and pCO_2 and SST had clear diel cycles (Figure 4a). The values of pCO_2 and SST had an afternoon maximum occurring between 14:00 and 15:00 of ~450 μatm and ~31°C, respectively, and a morning minimum occurring between 7:00 and 9:00 of ~437 μatm and ~30°C, respectively. The surface heating and cooling were prominent over a diel cycle. The daily pCO_2 cycle closely followed the daily temperature cycle (Figure 4a). After removing the temperature effect, n-pCO_2 showed little diel variation before the TEP, indicating that temperature was indeed the major driver of surface pCO_2 variations before Typhoon T1305. U_{10} also had a diel cycle before the typhoon, with the minimum occurring between 8:00 and 9:00 and the maximum occurring around 0:00, and with a range of 0–6 m s^{-1} (Figure 4b).

The TEP of Typhoon T1305 started in the afternoon of 20 June (Figure 4a). During the TEP, U_{10} increased from 5.9 m s^{-1} to a maximum of 19.4 m s^{-1} in 27 hr, while SST and pCO_2 decreased by ~1.2°C and ~20 μatm simultaneously with minimal changes in n-pCO_2 (Figure 4a). The typhoon thus had a pronounced cooling effect, which primarily caused the decrease of pCO_2 (Koch et al., 2009). Thereafter, U_{10} decreased from its maximum to about 8 m s^{-1} in 12 hr. During this period, SST and pCO_2 continued to decrease, while n-pCO_2 showed a slight increase of ~5 μatm. Immediately after the passage of this typhoon, on 23 June, U_{10}

Table 1
Summary Information of Three Typhoons in the Study

Typhoon	Date passing through the SCS	Radius of maximum wind speed (km) Min	Mean	Max	Wind speed ($m\ s^{-1}$) Min	Mean	Max	The nearest distance to the buoy (km)
T1305 Bebinca	20 Jun to 23 Jun	83	90	93	10.3	13.8	18.0	69
T1306 Rumbia	29 Jun to 2 Jul	19	62	83	18.0	24.1	36.0	251
T1309 Jebi	31 Jul to 3 Aug	37	70	111	15.4	22.3	30.9	382

Note. Radius of maximum wind speed is the distance between the typhoon center and the location of maximum wind.

still fluctuated around 9 $m\ s^{-1}$, while n-pCO_2 recovered to the pretyphoon value. Neither SST nor pCO_2 recovered to the pretyphoon levels on 19 and 20 June (Figure 4a).

Interestingly, the typhoon seemed to have a three-step effect (Figures 4a and 4b). The first step was mainly to lower the surface temperature, and thus surface pCO_2, with limited changes in n-pCO_2 (Figure 4a). In the second step, surface temperature and pCO_2 continued to decrease while n-pCO_2 was elevated. Thereafter, in the third step, n-pCO_2 decreased while temperature increased and in situ pCO_2 changed little. The plausible mechanisms of these changes may be the following: (1) As the typhoon moved into the area of the buoy, it caused surface water cooling, which in turn caused surface pCO_2 to decrease while n-pCO_2 changed little. (2) In the second step, water with relatively high CO_2 concentration was brought up from depth through vertical mixing and the surface water was continuous cooled. The cooling effect on pCO_2 probably exceeded the effect of the mixing and caused a net decrease of pCO_2. However, the vertical mixing seemed to elevate n-pCO_2 in the second step (Figure 4a). (3) In the third step, n-pCO_2 decreased, likely due to biological uptake stimulated by the nutrient supply from deep water. Meanwhile, pCO_2 changed little as a result of the balance between SST increase and biological activity. Unfortunately, no chlorophyll or fluorescence measurements were acquired during the typhoon periods, and satellite data were not available during these periods due to cloud coverage. However, the above interpretation is consistent with the observations, and explanations, from similar studies in the North Pacific and North Atlantic (Hood et al., 2001; Nemoto et al., 2009).

After the passage of T1305, pCO_2 was consistently more than 25 μatm lower than pretyphoon values. This pCO_2 decrease was accompanied by an SST decrease of 1.5°C. By calculation, this cooling effect alone corresponds to a pCO_2 decrease of 26 μatm, consistent with the observed pCO_2 decrease seen before and after the typhoon.

3.2.2. Typhoon Rumbia (T1306, 30 June to 3 July 2013)

The second typhoon, Typhoon Rumbia (T1306), entered the SCS on 30 June. Its center passed south of the buoy at a nearest distance of 251 km (Table 1). Before the passage of T1306, pCO_2 varied between 415 and 430 μatm and SST ranged from 28.92 to 29.74°C (Figures 4c and 4d). The diel cycles of SST and pCO_2 observed prior to T1306 were similar to those seen before T1305, while n-pCO_2 again varied little (Figure 4c). This typhoon also produced a three-step effect in pCO_2 during its TEP. First, U_{10} started increasing in the middle of June 30 (Figure 4d). Within 17 hr (first step), pCO_2 and SST decreased by 9 μatm and 0.65°C, respectively, while n-pCO_2 showed little change (Figure 4c). After U_{10} reached its maximum value (15.3 $m\ s^{-1}$) around 9:00 on 1 July (start of the second step), SST continued to decrease, while n-pCO_2 started to increase. However, pCO_2 changed little until early 2 July, after which it increased and reached ~430 μatm in the latter part of 2 July. SST began to recover in the middle of 2 July. This pattern was similar to that observed during Typhoon T1305, when cooling seemed to play a major role in controlling surface pCO_2 initially, and vertical mixing seemed to surpass the cooling effect later on. By 3 July, SST and pCO_2 had recovered to their pretyphoon values. In the third step, n-pCO_2 decreased by more than 10 μatm from 2 to 3 July, again probably an indication of elevated biological activity that seemed to be more prominent than that during Typhoon T1305.

3.2.3. Typhoon Jebi (T1309, 1–4 August 2013)

The effects of Typhoon T1309 were somewhat different from the previous two. On 30–31 July, before the passage of T1309, SST and pCO_2 again covaried and followed a similar diel pattern (Figure 4e). However, as

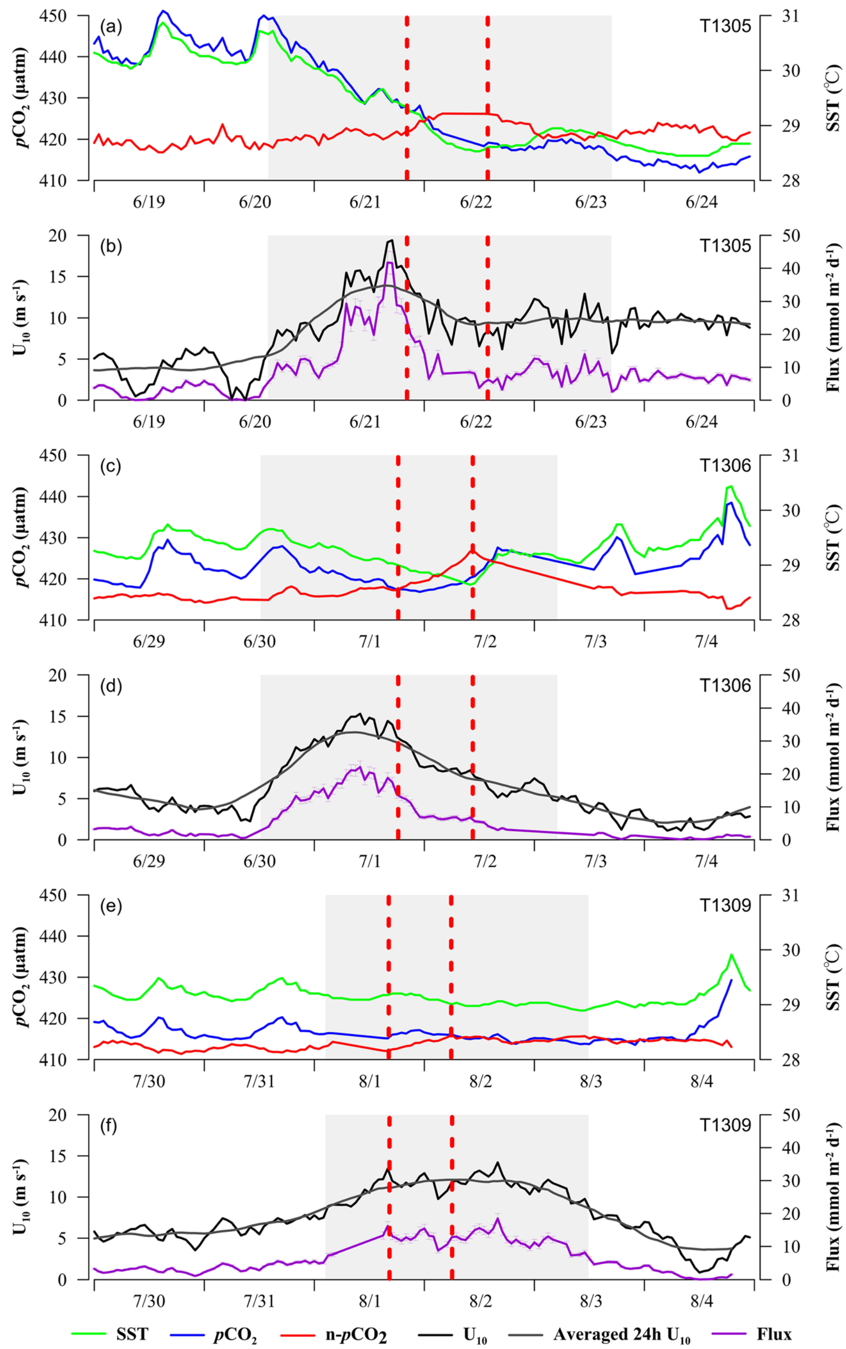

Figure 4. Variations of surface SST, pCO$_2$, n-pCO$_2$, U_{10}, and CO$_2$ flux before, during and after three typhoons: Typhoon T1305 (a and b), Typhoon T1306 (c and d), and Typhoon T1309 (e and f). Gray shaded areas represent TEPs. Red dashed lines mark the approximate separation of the three steps during each TEP where different typhoon effects on pCO$_2$ and n-pCO$_2$ occurred (see text).

opposed to what was observed prior to the previous two typhoons, n-pCO$_2$ also seemed to have a slight diel cycle before Typhoon T1309, with a n-pCO$_2$ minimum at around 16:00 and a maximum around 05:00 (Figure 4e). This was opposite to the pCO$_2$ diel pattern but was consistent with effects of biological activity in which net primary production drove n-pCO$_2$ to low values during the day while net respiration drove n-pCO$_2$ higher at night. The diel cycle of pCO$_2$ includes combined effects of SST, biology, and other factors, such as mixing. Before the typhoon, SST was still the major driver of surface pCO$_2$, as both

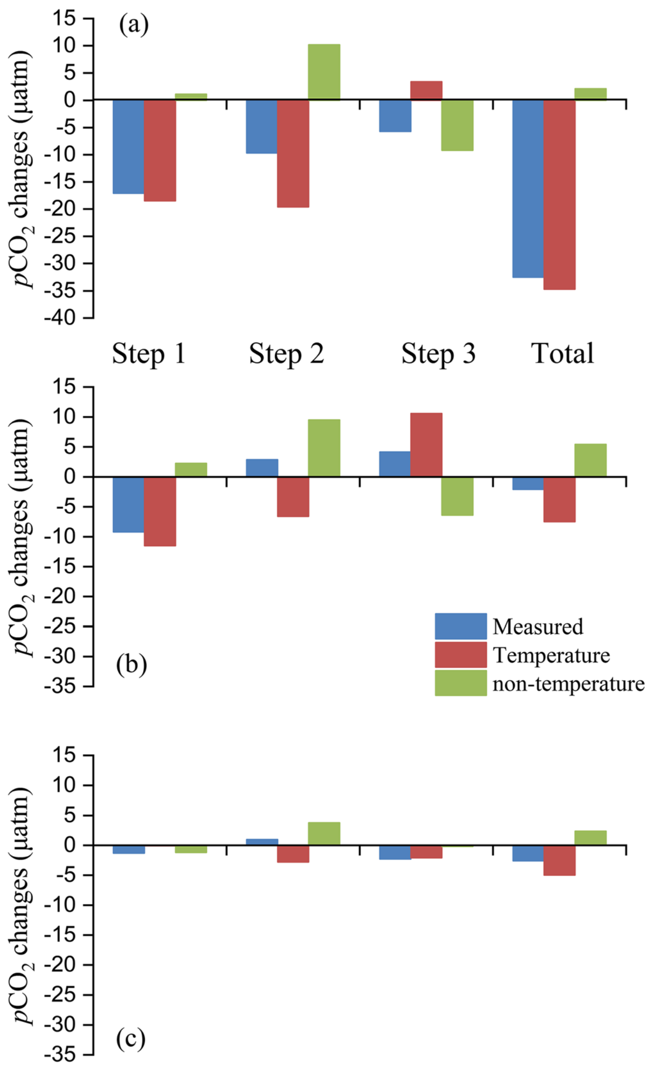

Figure 5. Contributions of temperature and nontemperature factors to surface $p\mathrm{CO_2}$ changes during Typhoons T1305 (a), T1306 (b), and T1309 (c). Each TEP was further divided into three steps as defined in Figure 4. Temperature effect was calculated from temperature changes between each step using temperature factor of 0.0423°C^{-1} (Takahashi et al., 1993). Nontemperature effect was calculated as the residuals between total change in $p\mathrm{CO_2}$ and change due to temperature effect. Total effect during each TEP was calculated as the sum of individual changes in three steps.

strongly covaried (Figure 4e). Starting on 1 August, U_{10} increased over 14 hr from ~7 m s^{-1} to a maximum of 14.2 m s^{-1} due to the typhoon. In the next 3 days, SST and $p\mathrm{CO_2}$ showed little diel variation and their values slightly decreased by ~0.29°C and ~4 μatm, respectively. In the meantime, n-$p\mathrm{CO_2}$ increased by ~4 μatm. There was no clear three-step effect produced by this typhoon. Because this typhoon passed no closer than 382 km from the buoy site, much farther than the closest approach of other two typhoons, the effects on SST and $p\mathrm{CO_2}$ were relatively small. On 4 August, the diel cycles of SST and $p\mathrm{CO_2}$ recovered but with a much larger range than before the storm.

3.2.4. Assessments of Typhoon Effects on $p\mathrm{CO_2}$

Even though the proposed three-step process is tentative, further assessments of the contributions of temperature and nontemperature factors on changes of surface $p\mathrm{CO_2}$ over TEPs may be helpful in supporting the three-step interpretation for Typhoons T1305 and T1306 (Figure 5). Even though there was not a clear three-step effect for Typhoon T1309 (Figure 4), we approximately categorized its three steps based on n-$p\mathrm{CO_2}$ for comparison: n-$p\mathrm{CO_2}$ had little change in the first step, and the second step started when n-$p\mathrm{CO_2}$ started to increase until the maximum, followed by the third step, which then concluded at the end of TEP.

For Typhoons T1305 and T1306, it is clear that in the first step decreasing temperature had a dominant effect on declining surface $p\mathrm{CO_2}$, while nontemperature factors (i.e., physical and biological factors) had a minor effect (Figure 5). In the second step, temperature still played an important role in changes in $p\mathrm{CO_2}$, but nontemperature factors, presumably vertical mixing (as no previous studies or data have suggested elevated biological activities during a cyclone), caused the $p\mathrm{CO_2}$ to increase significantly, with a magnitude similar to the temperature effect. The effect of these two factors counteracted each other, causing relatively small changes in $p\mathrm{CO_2}$. In the third step, temperature increase caused the increase of $p\mathrm{CO_2}$, while nontemperature factors, probably net biological uptake fueled by nutrient-rich water from depth, caused the decrease of $p\mathrm{CO_2}$. The net effect of temperature and biology in the third step caused a small change in $p\mathrm{CO_2}$. Enhanced biological production was also attributed to the decrease of $p\mathrm{CO_2}$ in the East China Sea and North Atlantic after typhoon passage (Hood et al., 2001; Nemoto et al., 2009). This study suggests, however, that surface $p\mathrm{CO_2}$ may not always decrease, depending on the balance of warming and enhanced primary production after typhoon passage. Overall, temperature was still likely the main factor controlling $p\mathrm{CO_2}$ for all typhoons, while nontemperature factors, that is, mixing and biology, might have accounted for a significant portion of $p\mathrm{CO_2}$ changes at times. It is also noted that vertical mixing and biology have opposite effects on surface $p\mathrm{CO_2}$, and thus, the net effect of the two might vary between typhoons (Figure 5).

The magnitude of the effects of these three typhoons on surface $p\mathrm{CO_2}$ is different (Figure 5). This is likely related to the distance between the typhoon track and the buoy sites, as well as the typhoon intensity. The maximum wind speed of T1305 was much lower than T1306 and T1309 (Table 1). But the radius of maximum wind speed of T1305 was larger than T1306 and T1309 (Table 1). The nearest distance between the typhoon track and the buoy site for T1305 was only ~69 km, much closer than the nearest distances of T1306 (~251 km) and T1309 (~382 km). Typhoon T1305 had the greatest influence on $p\mathrm{CO_2}$, followed by T1306 and T1309 (Figure 5). This indicates that the distance between the typhoon track and the buoy site was much more

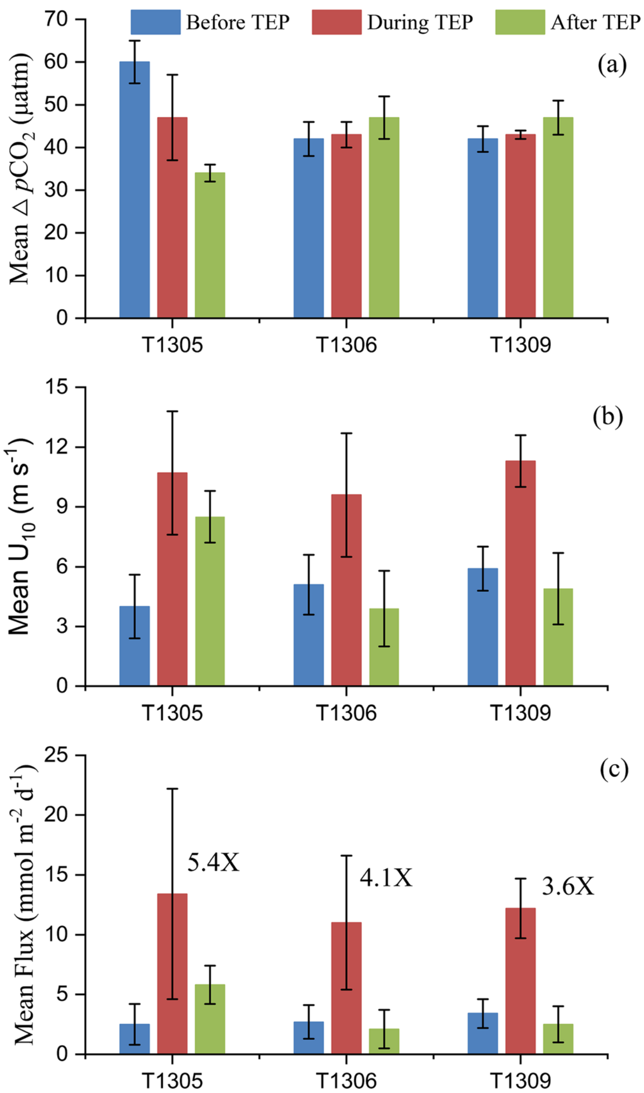

Figure 6. Comparison of mean ΔpCO_2 (a), mean U_{10} (b), and mean flux (c) before, during and after the TEP of three typhoons described in the text. Error bars are standard deviations. The numbers in (c) represent multiples of the mean CO_2 flux during the typhoon compared to the pretyphoon values.

important than the maximum typhoon wind speed. It is worth pointing out that the two buoy sites in this study were located at the northern SCS slope area, which is typically oligotrophic and low in productivity. This discussion is thus representative of the oligotrophic part of the SCS.

3.3. Effects of Typhoons on Air-Sea CO_2 Fluxes

The mean air-sea CO_2 flux excluding TEPs in the northern SCS during the study period was 3.9 ± 3.2 mmol m^{-2} day^{-1}, close to the value of 3.2 ± 0.3 mmol m^{-2} day^{-1} determined from summertime field surveys measurements from offshore water in the SCS (Zhai et al., 2013). During three TEPs, the CO_2 flux ranged from 3.0 (T1309) to 41.7 (T1305) mmol m^{-2} day^{-1}, with a mean of 11.0–13.4 mmol m^{-2} day^{-1}, which was about 3 times the mean flux under nontyphoon conditions. Generally, the air-sea CO_2 flux varied with wind speed (Figure 3). The highest flux occurred on the days when typhoons passed nearby the buoy, corresponding to the highest U_{10} (Figure 3). In contrast, the fluxes were low in May and June even though ΔpCO_2 of those months were the highest (the maximum value was 106 μatm) of the study period. Typhoons had a minor effect on pCO_2^{air} (Figure 3). Typhoons affect air-sea CO_2 fluxes mainly through their effects on pCO_2 and U_{10} (Figure 4). The typhoons in this study either reduced (T1305) or only slightly changed surface ΔpCO_2 (T1306 and T1309, Figure 6a). As such, the increase in CO_2 flux during typhoons resulted primarily from elevated U_{10} (Figures 6b and 6c).

The mean CO_2 fluxes before, during, and after each typhoon showed similar changes (Figure 6c). The flux was less than 4 mmol m^{-2} day^{-1} before the passage of each typhoon. The overall mean CO_2 flux was only 2.9 ± 0.5 mmol m^{-2} day^{-1} before the typhoons passage (determined over a period of time before each TEP with a length of thevTEP). However, the overall mean increased to 12.2 ± 1.2 mmol m^{-2} day^{-1} during TEPs (Figure 6c). After typhoons, it decreased to 3.5 ± 2.0 mmol m^{-2} day^{-1} (determined over a period of time following the TEP of length of the TEP), which was slightly higher than the values before typhoons. Mean CO_2 flux during TEPs amounted to 3.6 to 5.4 times pretyphoon values (Figure 6c), corresponding to a 1.9–2.7-fold increase in U_{10} from pretyphoon values. Overall, all three typhoons dramatically increased the magnitude of CO_2 efflux.

During each TEP, the maximum decrease of pCO_2 (maximum pCO_2 − minimum pCO_2) was 32 μatm for T1305, 11 μatm for T1306, and 3 μatm for T1309 (Figure 4). A strong linear correlation was seen between ΔpCO_2 and the minimum distance between the typhoon center and the buoy site (Figure 7). The surface CO_2 flux increase factor (the multiples of the mean CO_2 flux during TEP compared to the values before TEP) (Figure 6c) was also strongly correlated with the nearest distance to typhoon (Figure 7). The increase factor was not likely related to the strength of the typhoon, as all three typhoons were classified as *tropical storms* and were of similar intensity. Our results thus indicate that the effect of typhoons on CO_2 flux varies spatially, although additional studies are needed to fully assess this spatial variation.

In this study, the TEP lasted 75, 65 and 57 hr for Typhoons T1305, T1306, and T1309, respectively, totaling 197 hr, only 9% of the 94-day study period. The cumulative CO_2 efflux during the study period (Figure 8) shows significant influence of typhoons on the total CO_2 flux, which amounted to 429 mmol m^{-2} to the atmosphere over the 94 days. The cumulative CO_2 flux was 41, 26, and 28 mmol m^{-2} during T1305, T1306, and T1309, respectively. These totaled to 95 mmol m^{-2}, which equals 22% of the total CO_2 efflux

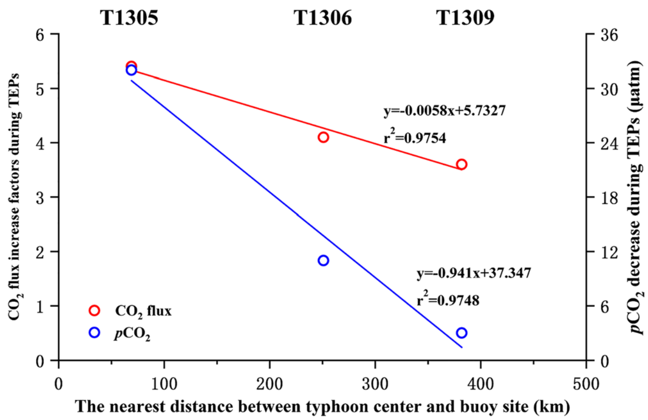

Figure 7. The nearest distance between three typhoon centers and the buoy site versus surface pCO_2 decrease and CO_2 flux increase factors (Figure 6c) during TEPs.

during the study period cited above. Zhai et al., 2013 estimated that the annual air-sea CO_2 flux was 460 ± 430 mmol m^{-2} year^{-1} in the northern SCS. This estimate was based on multiple underway surveys but did not consider the effect of typhoons on CO_2 flux. The CO_2 flux of these three typhoons correspondingly accounted for 21 ± 22% of the annual air-sea CO_2 flux estimated by Zhai et al.

The relative contribution of three typhoons to the total CO_2 flux (22%) in this study was not as high as the effect of cyclones in the East China Sea (60%) (Nemoto et al., 2009) and the Sargasso Sea (44%) (Bates et al., 1998). However, the magnitude of their contribution (95 mmol m^{-2}) was comparable to that of three typhoons in the East China Sea (90 mmol m^{-2}) (Nemoto et al., 2009). The CO_2 flux during the East China Sea typhoons constituted a larger fraction of the total flux because of the relatively small efflux of CO_2 flux from the East Chain Sea in the warm season (150 mmol m^{-2} from mid-July through mid-September, when that area acted as a CO_2 source). In the Sargasso Sea, three hurricanes contributed 145 mmol m^{-2} CO_2 flux from ocean to atmosphere, based on shipboard observations before and after the storms passed (Bates et al., 1998). Typhoons or hurricanes in the above study areas all increased CO_2 efflux. Although each storm is unique and can generate different effects on surface pCO_2 and CO_2 flux, all of the above studies found that the storm effect accounted for a significant portion of the total CO_2 flux during the study periods.

3.4. Interannual Variations of Typhoon's Impact on Air-Sea CO_2 Flux

Both the current study (Figure 3) and previous studies (Bates et al., 1998; Nemoto et al., 2009) indicate that air-sea CO_2 fluxes are mostly controlled by wind speeds, while the effect of the air-sea CO_2 gradient (ΔpCO_2) is secondary during tropical cyclones. This provides the capacity to estimate the interannual variability of the impact of typhoons on air-sea CO_2 flux in the northern SCS using only long-term wind and SST data products. Herein, to estimate a 10-year (2008–2018) time series of CO_2 flux near the buoy locations during TEPs, we used the long-term U_{10} and SST data from two well-established data repositories. The U_{10} data were extracted from the National Centers for Environmental Prediction (NCEP, https://www.ncep.noaa.gov) reanalysis data base. We utilized the U_{10} series (6-hr interval) from the NCEP grid cell encompassing the buoy locations, with its center 75 km from the centroid of the buoys. The U_{10} series from this cell aligns closely with U_{10} series derived from buoy measurements, capturing the primary temporal trends as well as the signal of the three principal typhoons (Figure 3d), although the strong winds of Typhoon T1305 appear in the NCEP series two days after they are seen in the in situ measurements. The SST data were obtained from the National Oceanic and Atmospheric Administration (NOAA) Earth Systems Research Laboratory (ERSL, https://www.esrl.noaa.gov/) daily averaged, optimally interpolated SST data base. The SST series from the 0.25° × 0.25° cell with the center closest (within 35 km) to the buoys' centroid was employed in the flux calculation. The SST series was first interpolated to the times of the U_{10} series. The ERSL SST series aligns well with the measured SSTs, although it does not capture the high-frequency (periods of a day or less) variability of the measured series (Figure 3b).

In modeling air-sea CO_2 flux during all TEPs with the 10-year SST and U_{10} series described above, we assumed an air-sea ΔpCO_2 of 44 μatm, which is equal to the mean ΔpCO_2 determined during the TEPs of our study (±7 μatm, SD). To estimate the yearly total CO_2 flux associated with the passage of typhoons, the yearly number of typhoons traversing the SCS was determined from the JTWC track data and the annual total TEP was calculated from the U_{10} data (section 2.3). For comparison, the modeled total CO_2 flux during three TEPs in 2013 was 105 mmol m^{-2}, which gave a difference of ~10% compared to the in situ measurements in this study (95 mmol m^{-2}). This suggests that our method of estimating CO_2 fluxes during TEPs is reasonable.

The estimates of the total accumulated annual air-sea CO_2 flux during the TEPs show considerable interannual variation, ranging from 104 to 259 mmol m^{-2} (164 mmol m^{-2} on average) (Figure 9d). Much of this

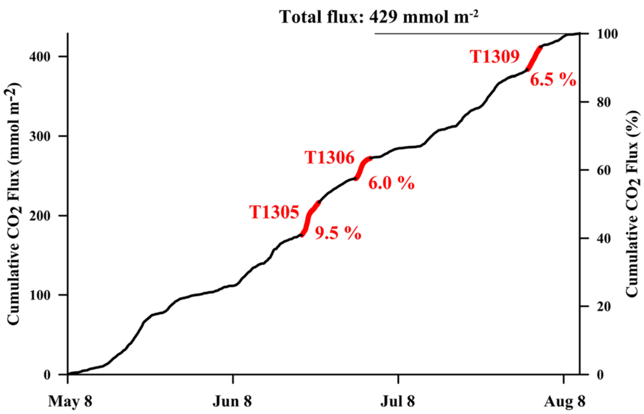

Figure 8. Cumulative CO_2 flux (the sum of hourly values) over the study period from 8 May through 10 August 2013. There were some gaps in the time series of pCO_2 and U_{10} and thus in the calculated CO_2 flux. We linearly interpolated the data to fill the gaps in order to calculate cumulative flux.

variation is due to the interannual variation in total TEP, U_{10}, and the number of typhoons (i.e., typhoon frequency) traversing the SCS. It is worth noting that no single factor among these has a dominant effect on CO_2 flux during TEPs (Figure 9). Locally, CO_2 efflux increases with the number of typhoons (Koch et al., 2009). Over 2008–2018, three to seven typhoons passed over the northern SCS annually (Figure 9a), while the annual total TEP associated with these typhoons ranged between 174 and 402 hr (Figure 9c). The annual averaged U_{10} during TEPs ranged between 9.6 and 13.8 m s^{-1} (11.9 m s^{-1} on average, Figure 9b), which was comparable to that observed on the buoy. Typhoon-enhanced air-sea CO_2 flux was highest in 2013 (Figure 9d), which had both higher U_{10} and total TEP.

Overall, the impact of typhoons in the northern SCS is shown to be significant relative to annual CO_2 fluxes and highly variable interannually. The above yearly estimated fluxes during the TEPs account for 23–56% (36% on average, Figure 9d) of the annual CO_2 flux (460 mmol m^{-2}, Zhai et al., 2013) from the northern SCS, while only 2.0–4.6% of time was categorized as TEP. The contribution of typhoons to annual air-sea CO_2 flux in most years of the last decade was between 30% and 45% (with the exceptions of 2013, ~56%, and 2014, ~23%) without an apparent long-term trend. Such large variability caused by typhoon's effects likely exerts an important

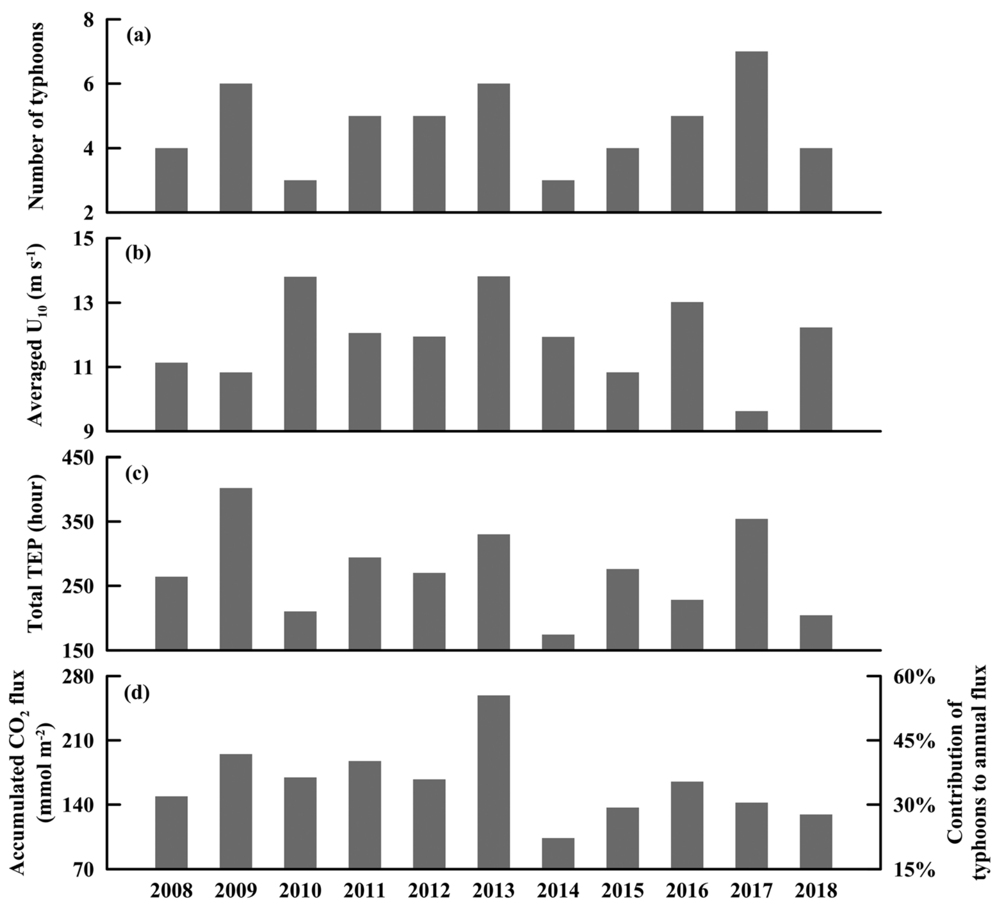

Figure 9. Interannual variability (2008–2018) of (a) number of typhoons traversing the northern SCS, (b) annual mean U_{10} during the TEPs, (c) the annual total TEP, and (d) the total accumulated air-sea CO_2 flux during the TEPs of each year (the left vertical axis represents the total values, and the right denotes the relative contribution to the annual total CO_2 flux).

control on interannual variability of the annual CO_2 flux budget in the region, as it is generally larger than the seasonal variability of CO_2 flux (Figure 3). As such, typhoons may play a major role of affecting air-sea CO_2 flux from the SCS over both short and long terms.

4. Conclusions

This study conducted an in-depth analysis on the effects of typhoons on surface $p\text{CO}_2$ and CO_2 fluxes in the northern SCS, the largest tropical marginal sea in the world. During the entire study period from May to August 2013, the study region was a source of CO_2 to the atmosphere. Under nontyphoon conditions, temperature generally played a primary role in controlling surface water $p\text{CO}_2$, including its daily cycle, while biological and physical effects were secondary, consistent with the study area as an oligotrophic tropical shelf region.

The study site was affected by three major typhoons during the study period. Their effects were reflected in both surface $p\text{CO}_2$ and CO_2 fluxes. The typhoons seemed to have a three-step impact on surface $p\text{CO}_2$, where the first step at the beginning period of a typhoon was to lower SST thus surface $p\text{CO}_2$ and the second step likely resulted from vertical mixing that brought up water with high CO_2 concentrations from depth. In the third step, this water, enriched in CO_2 and nutrients, likely triggered net biological CO_2 uptake that lowered surface $p\text{CO}_2$. Although temperature continued to play an important role in controlling surface $p\text{CO}_2$ during typhoon periods, mixing and biology seem to exert significant impacts on $p\text{CO}_2$ at times. Such a proposed multistep process is consistent with studies in other regions, although more detailed studies are required to further examine the mechanisms controlling changes in surface $p\text{CO}_2$.

The typhoons' effect on air-sea CO_2 flux occurred mainly through increased U_{10}, and thus greater CO_2 efflux, during each typhoon. The mean CO_2 flux during a typhoon observed in this study reached 3.6 to 5.4 times the pretyphoon mean flux. The magnitude of the typhoon effect was strongly correlated with the distance to typhoon center. The typhoon effect translated to about 22% of the total CO_2 flux during the study period, which was influenced by typhoons only 9% of the time. A long-term analysis revealed that the effect of typhoons accounted for 23–56% of the annual air-sea CO_2 efflux in the northern SCS during the last decade (2008–2018), indicating that typhoons substantially enhanced the flux of CO_2 to the atmosphere. Typhoons and other tropical cyclones thus likely play a major role in determining the annual CO_2 fluxes both in the short and long terms in the SCS and beyond. These results support the prediction that tropical cyclones will play an increasingly important role in controlling air-sea CO_2 fluxes in a warmer and stormier ocean.

Data Availability Statement

The data in this study are available online (at https://figshare.com/s/b9fa471ebd38442ca0ff).

Acknowledgments

The authors express their gratitude to the crew members of the research vessel *Huizhi* and to Tao Ding, Beifeng Zhou, and Ruzhou Dong for their assistance in deployment and technical support. We thank Mallory Ringham and Kate Morkeski for editing. We also express our gratitude to two anonymous reviewers for their insightful comments and suggestions. This study was supported by the Marine Public Welfare Project of China (Grant 200905012), the Scientific Research Fund of the Second Institute of Oceanography of China (Grant JT1502), the Global Change and Air-Sea Interaction project of China (Grant GASI-03-01-02-02), and the National Natural Sciences Foundation of China (Grant 91128212).

References

Bai, Y., Huang, T. H., He, X. Q., Wang, S. L., Hsin, Y. C., Wu, C. R., et al. (2015). Intrusion of the Pearl River plume into the main channel of the Taiwan Strait in summer. *Journal of Sea Research*, *95*, 1–15. https://doi.org/10.1016/j.seares.2014.10.003

Bates, N. R., Knap, A. H., & Michaels, A. F. (1998). Contribution of hurricanes to local and global estimates of air-sea exchange of CO_2. *Nature*, *395*(6697), 58–61. https://doi.org/10.1038/25703

Bauer, J. E., Cai, W. J., Raymond, P. A., Bianchi, T. S., Hopkinson, C. S., & Regnier, P. A. G. (2013). The changing carbon cycle of the coastal ocean. *Nature*, *504*(7478), 61–70. https://doi.org/10.1038/nature12857

Cai, W. J., Dai, M. H., & Wang, Y. C. (2006). Air-sea exchange of carbon dioxide in ocean margins: A province-based synthesis. *Geophysical Research Letters*, *33*, L12603. https://doi.org/10.1029/2006GL026219

Cai, W. J., Hu, X. P., Huang, W. J., Murrell, M. C., Lehrter, J. C., Lohrenz, S. E., et al. (2011). Acidification of subsurface coastal waters enhanced by eutrophication. *Nature Geoscience*, *4*(11), 766–770. https://doi.org/10.1038/NGEO1297

Cao, Z. M., Dai, M. H., Zheng, N., Wang, D. L., Li, Q., Zhai, W. D., et al. (2011). Dynamics of the carbonate system in a large continental shelf system under the influence of both a river plume and coastal upwelling. *Journal of Geophysical Research*, *116*, G02010. https://doi.org/10.1029/2010JG001596

Chang, Y., Liao, H. T., Lee, M. A., Chan, J. W., Shieh, W. J., Lee, K. T., et al. (2008). Multisatellite observation on upwelling after the passage of Typhoon Hai-Tang in the southern East China Sea. *Geophysical Research Letters*, *35*, L03612. https://doi.org/10.1029/2007GL032858

Chen, C. T. A., & Borges, A. V. (2009). Reconciling opposing views on carbon cycling in the coastal ocean: Continental shelves as sinks and near-shore ecosystems as sources of atmospheric CO_2. *Deep-Sea Research Part II: Topical Studies in Oceanography*, *56*(8–10), 578–590. https://doi.org/10.1016/j.dsr2.2009.01.001

Chen, C. T. A., Gao, X. L., Ishizaka, J., & Lebel, L. (2015). Coastal seas in a changing world: Anthropogenic impact and environmental responses. *Continental Shelf Research*, *111*, 109–111. https://doi.org/10.1016/j.csr.2015.11.007

Chen, C. T. A., Liu, C. T., Chuang, W. S., Yang, Y. J., Shiah, F. K., Tang, T. Y., & Chung, S. W. (2003). Enhanced buoyancy and hence upwelling of subsurface Kuroshio waters after a typhoon in the southern East China Sea. *Journal of Marine Systems*, *42*(1–2), 65–79. https://doi.org/10.1016/S0924-7963(03)00065-4

Chen, C. T. A., Wang, S. L., Chou, W. C., & Sheu, D. D. (2006). Carbonate chemistry and projected future changes in pH and $CaCO_3$ saturation state of the South China Sea. *Marine Chemistry*, *101*(3–4), 277–305. https://doi.org/10.1016/j.marchem.2006.01.007

Chen, C. T. A., Wang, S. L., Wang, B. J., & Pai, S. C. (2001). Nutrient budgets for the South China Sea basin. *Marine Chemistry*, *75*(4), 281–300. https://doi.org/10.1016/S0304-4203(01)00041-X

Chen, Y. L. L., & Chen, H. Y. (2006). Seasonal dynamics of primary and new production in the northern South China Sea: The significance of river discharge and nutrient advection. *Deep-Sea Research Part I: Oceanographic Research Papers*, *53*(6), 971–986. https://doi.org/10.1016/j.dsr.2006.02.005

Chou, W. C., Sheu, D. D. D., Chen, C. T. A., Wang, S. L., & Tseng, C. M. (2005). Seasonal variability of carbon chemistry at the SEATS time-series site, northern South China Sea between 2002 and 2003. *Terrestrial, Atmospheric and Oceanic Sciences*, *16*(2), 445–465.

Dai, M. H., Cao, Z. M., Guo, X. H., Zhai, W. D., Liu, Z. Y., Yin, Z. Q., et al. (2013). Why are some marginal seas sources of atmospheric CO_2? *Geophysical Research Letters*, *40*, 2154–2158. https://doi.org/10.1002/grl.50390

Dai, M. H., Lu, Z. M., Zhai, W. D., Chen, B. S., Cao, Z. M., Zhou, K. B., et al. (2009). Diurnal variations of surface seawater $p$$CO_2$ in contrasting coastal environments. *Limnology and Oceanography*, *54*(3), 735–745. https://doi.org/10.4319/lo.2009.54.3.0735

Dai, M. H., Zhai, W. D., Cai, W. J., Callahan, J., Huang, B. Q., Shang, S. L., et al. (2008). Effects of an estuarine plume-associated bloom on the carbonate system in the lower reaches of the Pearl River estuary and the coastal zone of the northern South China Sea. *Continental Shelf Research*, *28*(12), 1416–1423. https://doi.org/10.1016/j.csr.2007.04.018

Du, C., Liu, Z., Dai, M. H., Kao, S. J., Cao, Z. M., Zhang, Y., et al. (2013). Impact of the Kuroshio intrusion on the nutrient inventory in the upper northern South China Sea: Insights from an isopycnal mixing model. *Biogeosciences*, *10*(10), 6419–6432. https://doi.org/10.5194/bg-10-6419-2013

Guo, X. H., Cai, W. J., Zhai, W. D., Dai, M. H., Wang, Y. C., & Chen, B. S. (2008). Seasonal variations in the inorganic carbon system in the Pearl River (Zhujiang) estuary. *Continental Shelf Research*, *28*(12), 1424–1434. https://doi.org/10.1016/j.csr.2007.07.011

Han, W. Y. (1998). *Marine chemistry in the South China Sea* (p. 289). Beijing: Science Press. (in Chinese)

Han, W. Y., & Ma, K. M. (1988). Studies on the coastal upwelling along the coasts of the east Guangdong Province (in Chinese). *Acta Oceanography Sinica*, *10*(1), 52–59.

He, X. Q., Xu, D. F., Bai, Y., Pan, D. L., Chen, C. T. A., Chen, X. Y., & Gong, F. (2016). Eddy-entrained Pearl River plume into the oligotrophic basin of the South China Sea. *Continental Shelf Research*, *124*, 117–124. https://doi.org/10.1016/j.csr.2016.06.003

Ho, D. T., Law, C. S., Smith, M. J., Schlosser, P., Harvey, M., & Hill, P. (2006). Measurements of air-sea gas exchange at high wind speeds in the Southern Ocean: Implications for global parameterizations. *Geophysical Research Letters*, *33*, L16611. http://doi.org/10.1029/2006gl026817

Hood, E. M., Wanninkhof, R., & Merlivat, L. (2001). Short timescale variations of f (CO_2) in a North Atlantic warm-core eddy: Results from the Gas-Ex 98 carbon interface ocean atmosphere (CARIOCA) buoy data. *Journal of Geophysical Research*, *106*(C2), 2561–2572. https://doi.org/10.1029/1999JC000278

Huang, P. S., & Imberger, J. (2010). Variation of $p$$CO_2$ in ocean surface water in response to the passage of a hurricane. *Journal of Geophysical Research*, *115*, C10024. https://doi.org/10.1029/2010JC006185

Iida, Y., Kojima, A., Takatani, Y., Nakano, T., Sugimoto, H., Midorikawa, T., & Ishii, M. (2015). Trends in $p$$CO_2$ and air-sea CO_2 flux over the global open oceans for the last two decades. *Journal of Oceanography*, *71*(6), 637–661. https://doi.org/10.1007/s10872-015-0306-4

Intergovernmental Panel on Climate Change (IPCC) (2013). Summary for policymakers. In T. F. Stocker, D. Qin, G.-K. Plattner, M. Tignor, S. K. Allen, J. Boschung, et al. (Eds.), *Climate change 2013: The physical science basis. Contribution of Working Group I to the Fifth Assessment Report of the Intergovernmental Panel on Climate Change*. (7). Cambridge, United Kingdom and New York, NY, USA: Cambridge University Press.

Koch, J., McKinley, G. A., Bennington, V., & Ullman, D. (2009). Do hurricanes cause significant interannual variability in the air-sea CO_2 flux of the subtropical North Atlantic? *Geophysical Research Letters*, *36*, L07606. https://doi.org/10.1029/2009GL037553

Large, W. G., & Pond, S. (1981). Open ocean momentum flux measurements in moderate to strong winds. *Journal of Physical Oceanography*, *11*(3), 324–336. https://doi.org/10.1175/1520-0485(1981)011%3C0324:OOMFMI%3E2.0.CO;2

Laruelle, G. G., Lauerwald, R., Pfeil, B., & Regnier, P. (2014). Regionalized global budget of the CO_2 exchange at the air-water interface in continental shelf seas. *Global Biogeochemical Cycles*, *28*, 1199–1214. https://doi.org/10.1002/2014GB004832

Lin, I., Liu, W. T., Wu, C. C., Wong, G. T. F., Hu, C. M., Chen, Z. Q., et al. (2003). New evidence for enhanced ocean primary production triggered by tropical cyclone. *Geophysical Research Letters*, *30*(13), 1718. https://doi.org/10.1029/2003GL017141

Nemoto, K., Midorikawa, T., Wada, A., Ogawa, K., Takatani, S., Kimoto, H., et al. (2009). Continuous observations of atmospheric and oceanic CO_2 using a moored buoy in the East China Sea: Variations during the passage of typhoons. *Deep-Sea Research Part II: Topical Studies in Oceanography*, *56*(8–10), 542–553. https://doi.org/10.1016/j.dsr2.2008.12.015

Shang, S. L., Li, L., Li, J., Li, Y. H., Lin, G., & Sun, J. (2012). Phytoplankton bloom during the northeast monsoon in the Luzon Strait bordering the Kuroshio. *Remote Sensing of Environment*, *124*, 38–48. https://doi.org/10.1016/j.rse.2012.04.022

Sheu, W. J., Wu, C. R., & Oey, L. Y. (2010). Blocking and westward passage of eddies in the Luzon Strait. *Deep-Sea Research Part II: Topical Studies in Oceanography*, *57*(19–20), 1783–1791. https://doi.org/10.1016/j.dsr2.2010.04.004

Su, J. (2004). Overview of the South China Sea circulation and its influence on the coastal physical oceanography outside the Pearl River Estuary. *Continental Shelf Research*, *24*(16), 1745–1760. https://doi.org/10.1016/j.csr.2004.06.005

Sun, Q. Y., Tang, D. L., Legendre, L., & Shi, P. (2014). Enhanced air-sea CO_2 exchange influenced by a tropical depression in the South China Sea. *Journal of Geophysical Research: Oceans*, *119*, 6792–6804. https://doi.org/10.1002/2014JC010131

Sweeney, C., Gloor, E., Jacobson, A. R., Key, R. M., McKinley, G., Sarmiento, J. L., & Wanninkhof, R. (2007). Constraining global air-sea gas exchange for CO2 with recent bomb 14C measurements. *Global Biogeochemical Cycles*, *21*, GB2015. https://doi.org/10.1029/2006GB002784

Takahashi, T., Olafsson, J., Goddard, J. G., Chipman, D. W., & Sutherland, S. C. (1993). Seasonal variation of CO_2 and nutrients in the high-latitude surface ocean: A comparative study. *Global Biogeochemical Cycles*, *7*(4), 843–878. https://doi.org/10.1029/93gb02263

Takahashi, T., Sutherland, S. C., Wanninkhof, R., Sweeney, C., Feely, R. A., Chipman, D. W., et al. (2009). Climatological mean and decadal change in surface ocean $p$$CO_2$, and net air-sea CO_2 flux over the global oceans. *Deep-Sea Research Part II: Topical Studies in Oceanography*, *56*(8–10), 554–577. https://doi.org/10.1016/j.dsr2.2008.12.009

Tseng, C. M., Wong, G. T. F., Chou, W. C., Lee, B. S., Sheu, D. D., & Liu, K. K. (2007). Temporal variations in the carbonate system in the upper layer at the SEATS station. *Deep-Sea Research Part II: Topical Studies in Oceanography*, *54*(14–15), 1448–1468. https://doi.org/10.1016/j.dsr2.2007.05.003

Wanninkhof, R. (1992). Relationship between wind speed and gas exchange over the ocean. *Journal of Geophysical Research*, *97*(C5), 7373–7382. http://doi.org/10.1029/92jc00188

Wanninkhof, R. (2014). Relationship between wind speed and gas exchange over the ocean revisited. *Limnology and Oceanography: Methods*, *12*(6), 351–362. https://doi.org/10.4319/lom.2014.12.351

Wanninkhof, R., Park, G. H., Takahashi, T., Sweeney, C., Feely, R., Nojiri, Y., et al. (2013). Global ocean carbon uptake: Magnitude, variability and trends. *Biogeosciences*, *10*(3), 1983–2000. https://doi.org/10.5194/bg-10-1983-2013

Weiss, R. F. (1974). Carbon dioxide in water and seawater: The solubility of a non-ideal gas. *Marine Chemistry*, *2*(3), 203–215. https://doi.org/10.1016/0304-4203(74)90015-2

Wong, G. T. F., Ku, T. L., Mulholland, M., Tseng, C. M., & Wang, D. P. (2007). The SouthEast Asian time-series study (SEATS) and the biogeochemistry of the South China Sea—An overview. *Deep-Sea Research Part II: Topical Studies in Oceanography*, *54*(14–15), 1434–1447. https://doi.org/10.1016/j.dsr2.2007.05.012

Zhai, W. D., Dai, M. H., Cai, W. J., Wang, Y. C., & Hong, H. S. (2005). The partial pressure of carbon dioxide and air-sea fluxes in the northern South China Sea in spring, summer and autumn. *Marine Chemistry*, *96*(1–2), 87–97. https://doi.org/10.1016/j.marchem.2004.12.002

Zhai, W. D., Dai, M. H., Chen, B. S., Guo, X. H., Li, Q., Shang, S. L., et al. (2013). Seasonal variations of air-sea CO_2 fluxes in the largest tropical marginal sea (South China Sea) based on multiple-year underway measurements. *Biogeosciences*, *10*(11), 7775–7791. https://doi.org/10.5194/bg-10-7775-2013

Zhao, H., Tang, D. L., & Wang, Y. Q. (2008). Comparison of phytoplankton blooms triggered by two typhoons with different intensities and translation speeds in the South China Sea. *Marine Ecology Progress Series*, *365*, 57–65. https://doi.org/10.3354/meps0741838